JOURNAL OF FORENSIC SCIENCES

J Forensic Sci, January 2011, Vol. 56, No. 1
doi: 10.1111/j.1556-4029.2010.01562.x
Available online at: interscience.wiley.com

TECHNICAL NOTE

CRIMINALISTICS

Vinesh Rana,[1] *M.A.; Maria V. Cañamares,*[2] *Ph.D.; Thomas Kubic,*[1] *Ph.D.; Marco Leona,*[3] *Ph.D.; and John R. Lombardi,*[2] *Ph.D.*

Surface-enhanced Raman Spectroscopy for Trace Identification of Controlled Substances: Morphine, Codeine, and Hydrocodone

ABSTRACT: We obtain the normal Raman and surface-enhanced Raman spectrum of three controlled substances: morphine, codeine, and hydrocodone. The spectra are assigned with the aid of density functional theory. Because of rather intense fluorescence, normal Raman spectra suffer from poor signal-to-noise, even when differential subtraction techniques are employed. On the other hand, surface enhancement by Ag nanoparticles both enhances the Raman signal and suppresses the fluorescence, enabling far more sensitive detection and identification. We also present a set of discriminant bands, useful for distinguishing the three compounds, despite the similarities in their structures.

KEYWORDS: forensic science, Raman, SERDS, SERS, opiates, morphine, codeine, hydrocodone

In the past few years, Raman spectroscopy has become an important analytical technique in forensic laboratories because it provides a rapid and nondestructive method for trace detection. It is often preferred over infrared (IR) spectroscopy because aqueous solutions can be analyzed, unlike IR where aqueous solutions will have strong interfering water absorption bands. Another attractive feature of Raman spectroscopy is the ability to acquire spectra through certain container walls, such as glass bottles and various forms of packaging. Raman spectroscopy is obtained by the interaction if laser light with the dipole moment of a molecule (1). The resulting scattered light is shifted in frequency from that of the original light source, and the magnitude of the resulting shift is recorded as the Raman spectrum. One major problem that arises in utilizing Raman spectroscopy for forensic work is that normal Raman spectroscopy is quite weak and often obscured by fluorescence (2). Hence, surface-enhanced Raman scattering (SERS; [3]) is currently being explored for trace identification because it is more sensitive than traditional Raman scattering by 6–8 orders of magnitude. Furthermore, because of radiationless deactivation at the metal surface, fluorescence is quenched.

The use of the SERS technique requires the preparation of roughened surfaces of silver, gold, or copper or the use of silver or gold colloids. Because of the high sensitivity of SERS for aromatic systems (10^{-9} to 10^{-12} M), it is an ideal choice for the detection and identification of minute samples of controlled substances, textile dyes, inks, and explosives. In all these cases, only small samples are required for the SERS analysis. This results in minimal damage to the bulk of the original sample. Therefore, SERS provides a valuable method of detection that can be utilized in forensic laboratories where there is little control of the submitted sample and these are often very small.

The potential of SERS especially in forensic science, fields of trace evidence, the analysis of sub-milligram size samples of controlled substances, and questioned documents has been recently highlighted in a review of analytical tools for forensic science (1). Research so far has shown that SERS can be effectively applied to problems, such as the discrimination of jet printer inks *in situ* (4), inks from ball point pens (5), the rapid identification of synthetic dyes on fiber samples (6), the sensitive determination of narcotics (7), and other controlled substances (8), such as amphetamines (9), cocaine, and nicotine (10). Normal Raman spectra of morphine hydrochloride (11) and codeine phosphate (12) have been previously reported, as well as the SERS spectrum of codeine using a silver surface formed photolytically by the probe laser as the SERS substrate (13).

Since the early 1800s, opiates have been abused by humans because they are found in nature, and give a feeling of euphoria, but unfortunately they cause dependence. They also can be found in the medicinal world as narcotic analgesics. Opiates are divided into three categories: natural, semi-synthetic, and synthetic. The natural opiates are found in opium poppies, while the semi-synthetic and synthetic opiates are derived from the natural sources. Examples of natural opiates are morphine and codeine, while examples of semi-synthetic opiates are heroin, hydrocodone, and oxycodone. Methadone, on the other hand, is an example of a synthetic opiate. In this research, we concentrate on morphine (Fig. 1*a*), codeine (Fig. 1*b*), and hydrocodone (Fig. 1*c*), as they are commonly used opiates (14).

The purpose of this research is to examine the spectra of the opiates mentioned earlier using SERS and normal Raman

[1]Department of Forensic Science, John Jay College of Criminal Justice, 445 West 59th Street, New York, NY 10019.
[2]Department of Chemistry and Center for Study of Structures and Interfaces (CASI), The City College of New York, Convent Avenue at 138th Street, New York, NY 10031.
[3]Department of Scientific Research, The Metropolitan Museum of Art, 1000 Fifth Avenue, New York, NY 10028.

Received 21 Nov. 2008; and in revised form 28 Aug. 2009; accepted 15 Oct. 2009.

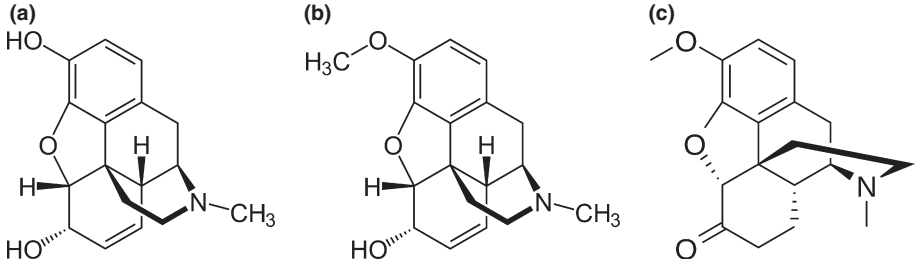

FIG. 1—*Structure of morphine (a), codeine (b), and hydrocodone (c).*

spectroscopy. In this study, we use silver colloids as SERS substrates because they give optimum enhancement in the visible to near-IR region. The experimental data was analyzed using density functional theory (DFT) calculations. DFT is a calculation of molecular structures and spectra obtained minimizing the total energy of the ground state of the molecule as a function of the electron density. DFT has the power to provide excellent values for normal mode vibrational frequencies and intensities. In recent works (15–18), we have found that DFT gives reliable and accurate way to predict and therefore to assign the Raman bands of various dye molecules. DFT has grown in popularity in computational chemistry because the calculations provide much better agreement with experimental values than the Hartree–Fock procedures (19). DFT calculations have been used before for the spectroscopic study of the interactions of the drug cocaine with other opiates, such as heroin and morphine (11).

Experimental

In this study, DEA-exempt, Quik-Chek™ opiate solutions (hydrocodone [018063], codeine [018013] and morphine [018033]) were obtained from Alltech Applied Science (Nicholasville, KY). These samples were supplied in methanol solution with a concentration of 1 mg/mL. The opiates used are in free base form.

Silver colloids were prepared following the method of Lee and Meisel (20) by reduction of silver nitrate (Aldrich 209139 Silver Nitrate 99.9%; Sigma-Aldrich, St. Louis, MO) with sodium citrate (Aldrich W302600 Sodium Citrate Dihydrate). The colloid thus obtained had a maximum absorption at 406 nm, when diluted 1:10 to maintain absorbance within instrumental range. The colloids were preconcentrated by centrifugation (2 min at $550 \times g$) prior to aggregation. The following solutions of different aggregating agents were prepared: NaCl 0.5 M, HCl 2 M, KNO_3 0.5 M, and NaOH 0.1 M. These aggregating agents enhance the formation of Ag clusters and produce a large surface area (21) for the exciting laser.

All solutions were prepared with ultrapure water. Glassware was thoroughly cleaned with a detergent, rinsed with ultrapure water, and finally in acetone and methanol.

Normal Raman spectra were obtained directly from crystals obtained via evaporation of the DEA-exempt drug solutions. One or two drops of the solution were placed on a clean microscope slide. After a few seconds of heating at 65°C, the methanol evaporated leaving behind the drug crystals. The slide was placed under a microscope and examined using a 100× objective. Two to three crystals of the drug were used to obtain the spectra.

For the SERS experiments, a 2-μL drop of 0.5 M NaCl was added to a precleaned microscope slide followed by 2 μL of the drug solution. Finally, a microliter of the Ag colloid solution was added and then viewed with the microscope to assure that the aggregation was accomplished. A Raman spectrum of the aggregated colloid, prior to adsorption of molecules to be studied has been previously published (16). Except for the low lying, intense 230/cm line and several weak citrate lines, it is found to provide little interference with the observed SERS spectra. Furthermore, it was found that the presence of cutting agents has no effect on our results as they have no discernable SERS spectrum.

Dispersive Raman Spectra

Both normal Raman and SERS spectra were obtained with a Bruker Senterra Raman microscope (Bruker Optics Inc., Billerica, MA) with 785 nm excitation, a 1200 rulings/mm holographic grating, and employing a charge-coupled device (CCD) detector. Additionally, a 633 nm laser in connection with a 1800 rulings/mm grating was also used. The spectral resolution was 3–5/cm. The acquisition time was 30 sec. To avoid sample damage, the power was kept at 25 mW for the normal Raman spectra collection at 785 nm. For the SERS analysis, the maximum power used was 100 and 20 mW for the 785- and 633-nm laser, respectively.

When using the 785-nm diode laser for the normal Raman analysis of the samples, some fluorescence was observed. The elimination of the fluorescence emission was carried out by a technique in which a Raman spectrum is collected with two slightly different excitation wavelengths, subtracted, and then integrated to form one spectrum. This technique is also known as shifted excitation Raman difference spectroscopy (SERDS; [22,23]). At 785 nm, the injection current to laser diode is modulated to produce alternation between two oscillating modes, following a procedure suggested by Maiwald et al. (24). The modes are separated by about 8/cm, and the difference spectrum is recorded on a CCD detector. The resulting spectrum resembles a derivative spectrum and to obtain the normal Raman spectrum, the derivative spectrum is integrated. To further reduce the noise introduced in the spectra by the SERDS technique, a 10-point FFT filter smoothing was carried out on the normal Raman spectra. Considerable reduction of background fluorescence can be obtained from this technique, and numerous weak lines, which normally are overwhelmed by the fluorescence, are elucidated. In Fig. 2*a*,*b*, we illustrate the advantage of SERDS in comparison with normal Raman spectroscopy for the Raman spectrum of morphine. For more details and typical results, see Maiwald et al. (24).

Calculations

Density functional calculations are carried out by assuming that the energy of a molecule is a functional of the electron density. The energy is then minimized with respect to the density, and an optimized structure may then be obtained. The geometry is optimized to a minimum total energy and then the Raman and IR frequencies were obtained. The Raman and IR frequencies are

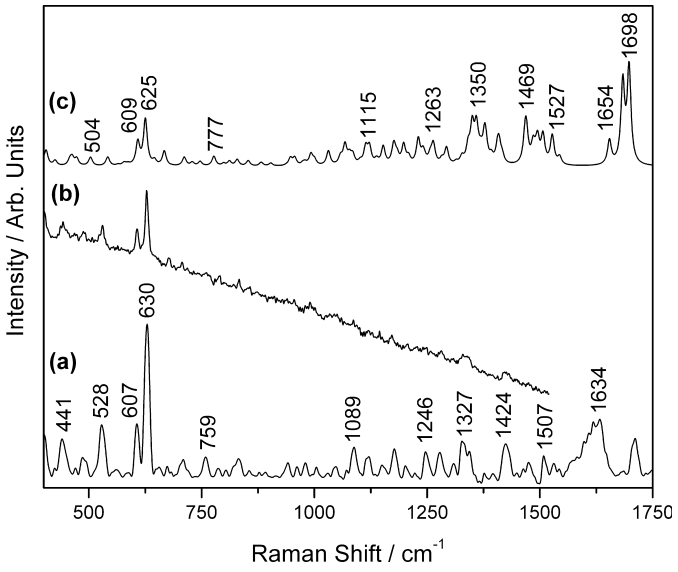

FIG. 2—*Normal Raman (comparison of the SERDS (a) and non-SERDS (b)) and calculated DFT (c) spectra of morphine.*

obtained by determining the variation of the energy with respect to imposed molecular displacements. DFT calculations were performed with Gaussian 03 (25) at the B3LYP level of theory and employing the 6–31+G (d,p) basis set. This basis set was chosen on the basis of earlier work, as the fit obtained is generally found to be excellent. In previous work on the flavones (16) and the alkaloid berberine (18), we found convincing fits to the observed spectra, despite the rather large size of the molecules. The vibrational normal mode assignments are based on the best-fit comparison of the calculated Raman spectrum with the observed normal Raman spectrum, without the necessity of scaling the calculated wavenumbers. A slight drift of the deviation with increasing wavenumber is to be expected in such calculations because of higher errors in correlation corrections. However, typical standard deviations of the fits are 10–15/cm, which are on the order of 1% of the calculated wavenumbers. The rather remarkable coincidence of intensities adds further credence to the proposed normal mode assignments. The DFT spectral calculations typically predict many more lines than are usually observed in spectra. Most of these lines are too weak to be observed and we have not reported them. However, some of these are listed in the tables because they might be expected to possess sufficient intensity to be observed, although we could not clearly detect them. The DFT calculations are carried out assuming the molecule is isolated (i.e., in the gas phase) while the normal Raman spectra are taken in the powder (or crystalline) form, and therefore we expect some differences in the intensities as well as the frequencies of some of the lines. Given these differences, it is remarkable that the results are as in close agreement as they are.

Results

Morphine

The comparison of the normal Raman (SERDS—lower trace) and DFT spectrum (upper trace) of morphine is shown in Fig. 2. A very good fit (SD $\sim$ 1%) is seen between the experimental and calculated Raman spectra, especially in the most intense region of the Raman spectrum (around 630/cm). In the high wavenumbers region, the bands in the DFT spectrum appear at higher values than

TABLE 1—*Wavenumbers of the DFT, normal Raman, and SERS spectra of morphine and assignments of vibrational normal modes.*

Description*	DFT	Raman	SERS
$\delta_r(CH_2)_B$, $\delta_r(CH_3)$, $\delta_w(CH_2)_D$, δ(CNC), δ(CCC)	462	441	443
$\delta(CH)_{A/C}$, $\gamma(CC)_C$, δ(CNC), δ(CCC), δ(C–OH)	504	486	
$\gamma(CC)_C$, $\delta(CH)_{A/C}$, δ(CCC), δ(CNC), δ(COC), $\delta_r(CH_2)$	542	528	531
$\gamma(CC)_C$, $\delta(CH)_C$, δ(CCC), δ(C–OH), $\delta_r(CH_2)$	609	607	607
$\delta(CH)_{A/C}$, $\gamma(CC)_C$, δ(CCC), δ(COC), δ(C–OH)	625	630	628
$\gamma(CH)_A$, δ(CCC), δ(COC)	667	674	671
		702	703
$\delta(CH)_A$, δ(CCC), δ(CNC)	712	710	
$\delta_r(CH_2)$, $\gamma(CC)_C$, $\gamma(CH)_C$, ν(CNC), δ(OH), δ(CCC)	777	756	
$\delta_r(CH_2)$, $\delta(CH)_C$, $\delta_r(CH_3)$, ν(C–OC), δ(CCC)	1031		1035
$\delta(CH)_C$, δ(OH), $\nu(N–CH_3)$, ν(C–OH), δ(CCC)	1115	1089	
$\delta(CCC)_C$, $\delta(CH)_C$, δ(OH), $\delta_s(CH_2)$	1230		1226
$\nu(CC)_C$, $\delta(CH)_C$, $\delta_s(CH_2)$, δ(OH)	1263	1276	1283
			1318
$\nu(CC)_C$, $\delta(CH)_C$, δ(CH), δ(OH), $\delta_w(CH_2)$	1350	1327	1348
			1370
			1423
$\delta_s(CH_2)_D$, $\delta(CH_3)_D$	1469	1424	1444
$\delta_s(CH_2)_D$, $\delta(CH_3)_D$	1527	1507	1525
$\nu(C=C)_A$	1698	1634	1627

*ν, stretching; δ, bending, γ, out-plane bending, δ_s, scissoring, δ_w, wagging, δ_r, rocking.

in the experimental one. This is most likely due to the fact that the molecule is considered to be in the vacuum for the calculations, while the Raman measurement was recorded from the drug in powder. The frequencies of the main bands and the assigned vibrational normal modes are shown in Table 1. The DFT Raman spectrum of morphine hydrochloride has been calculated previously by Garrido et al. (11). Although they have carried out the calculations of the salt form of the morphine drug, our results agree with theirs, taking into account that no scaling of the calculated wavenumbers was performed in our work.

In the normal Raman spectrum of morphine (Fig. 2*a*), intense bands are seen at 441, 528, 607, 630, 1327, 1424, and 1634/cm. When compared with the DFT-calculated spectra, those bands appear at 462, 542, 609, 625, 1350, 1469, and 1698/cm. These bands are assigned to vibrations of bonds in different parts of the drug (Table 1). For example, the most intense band, at 630/cm, mainly corresponds to the out of plane bending of the =C–H bonds in ring A ($\gamma(CH)_A$) with contributions of $\gamma(CH)_C$ and $\gamma(CC)_C$. On the other hand, the bands at 528 and 607/cm are assigned to out of plane deformations of the aromatic ring C, together with γ(CH) in rings A and C, and deformations of the skeleton forming the rings. The most intense band in the high wavenumber region, which appears at 1634/cm, corresponds to the stretching motion of the C=C bond in ring A ($\nu(C=C)_A$). FT-Raman bands of morphine sulfate have previously been reported by Schulz et al. (26) at 631, 1620, and 1642/cm. On the other hand, the normal Raman bands of morphine hydrochloride at 514 nm were reported (11) at 632, 775, 1066, 1347, 1419, and 1635/cm. These results agree reasonably well with those observed in our work.

For the SERS analysis of morphine, both the 785 and 633 nm lasers were employed to determine which gives the better spectrum. In this case, the 633 nm laser was superior because it gave a more intense spectrum with better signal/noise (Fig. 3). It can be seen that the relative intensity of the bands changes from the normal Raman to the SERS spectrum, because of the interaction of morphine with the Ag nanoparticles.

For example, the bands around 630/cm are no longer the most intense in the SERS spectrum, and some bands in the 1200–

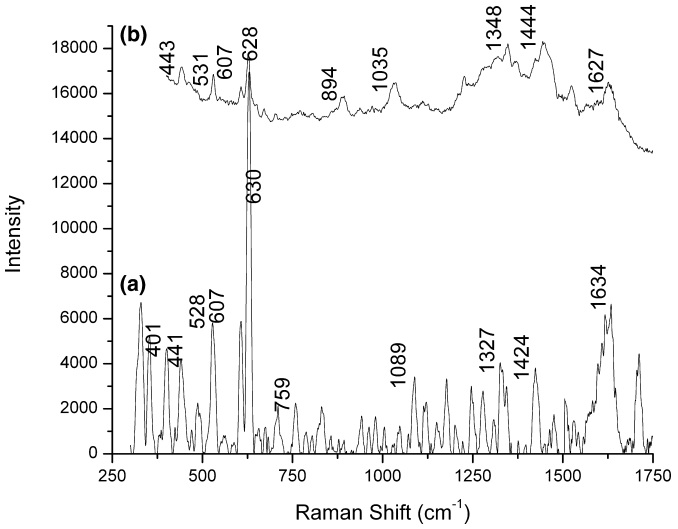

FIG. 3—*Normal Raman (SERDS at 785 nm) (a) and SERS (at 633 nm) (b) spectra of morphine.*

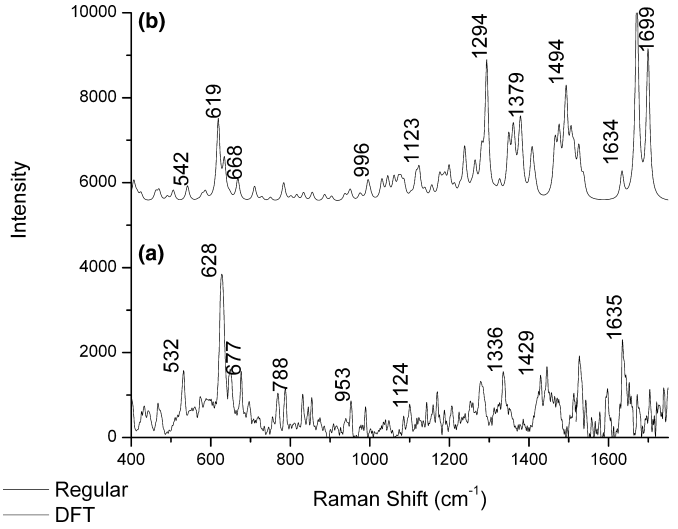

FIG. 4—*Normal Raman (SERDS) (a) and calculated DFT (b) spectra of codeine.*

1550/cm region, such as the ones at 1226, 1283, 1348, 1444, and 1525/cm, are greatly enhanced by the Ag surface. The band at 1230/cm is assigned to δ(CCC), δ(CH), δ(OH), and $\delta(CH_2)$ (Table 1). The same can be said of those at 1283 and 1348/cm, with the difference involving the ν(CC) motion instead of the δ(CCC) vibration. However, the vibration of the CH_2 group assigned to the 1283 and 1348/cm bands is different. The former involves a scissoring motion and the latter a wagging. The last two enhanced bands, at 1444 and 1525/cm correspond to deformations of the CH_2 and CH_3 groups in the D ring.

On the other hand, the band at 1627/cm, assigned to the ν(C=C) in the A ring, decreases relatively in intensity when the opiate is on the Ag surface. This band is also shifted from 1634 to 1627/cm in the SERS spectrum, showing a decrease in the strength of the double bond. These two facts, together with the decrease in the bands assigned to the $\delta(CH)_A$, suggest an interaction of morphine with the Ag through the C=C of the A ring. Our results are in agreement with those recently reported on a Ag island film at 633 nm by Li et al. (27).

The use of various aggregating agents, such as NaCl, HCl, KNO_3, and NaOH, was evaluated to determine which gives the highest enhancement at 785 nm. The acidic and neutral solutions showed similar SERS spectra. On the other hand, the basic solution showed diminished intensity in the lower wavenumber region.

Codeine

Figure 4 shows the normal Raman (*a*) and DFT-calculated spectrum (*b*) of codeine. As in the case of morphine, a very good fit is seen between the experimental and calculated Raman spectra, with the exception of the high wavenumber region. The normal Raman spectrum of codeine (Fig. 4*a*) shows the main bands at 532, 628, 650, 677, 1279, 1336, 1445, and 1635/cm. The corresponding calculated wavenumbers appear at 542, 619, 634, 668, 1294, 1349, 1494, and 1671/cm. The most intense band in the codeine Raman spectrum, which appears at 628/cm, and its shoulder at 650/cm, are assigned mainly to out of plane deformations, such as γ(CC), $\gamma(CH)_C$, and $\gamma(CH)_A$. However, the mid-intense Raman bands at 1279, 1336, and 1445/cm correspond to deformations of the carbon rings, and the characteristic bending motions of the CH, CH_2, and CH_3 groups. On the other hand, the bands in the 1600/cm region involve stretching motions of the C=C in ring A and of the carbons in the aromatic ring C. The complete list of the frequencies of the Raman bands and their assignments is shown in Table 2.

According to Schulz et al. (26), the FT-Raman spectrum of codeine shows bands at 628 and 1632/cm, which are also observed in our work. Good correspondence has been found between our result and the one obtained with excitation at 633 nm (12).

TABLE 2—*Wavenumbers of the DFT, normal Raman, and SERS spectra of codeine and assignments of vibrational normal modes.*

Description*	DFT	Raman	SERS
		433	443
$\gamma(CH)_A$, δ(CCC), δ(CNC), $\delta_r(CH_2)$	470	468	
$\gamma(CH)_{A/C}$, $\gamma(CC)_C$, δ(CNC), $\delta_r(CH_2)$, δ(COC)	542	532	530
$\gamma(CC)_C$, γ(CH), δ(OH), δ(COC), $\delta_s(CH_2)_B$	587		595
$\gamma(CC)_C$, $\gamma(CH)_{C/A}$, δ(CCC), δ(COC), δ(OH), $\delta_r(CH_2)_B$	619	628	629
$\gamma(CH)_{A/C}$, $\gamma(CC)_C$, δ(COC), $\delta_r(CH_2)$,	634	650	650
$\gamma(CH)_A$, δ(CCC), δ(COC)	668	677	674
$\gamma(CH)_A$, δ(CCC), δ(CNC), δ(COC), $\delta_r(CH_2)$, $\delta_r(CH_3)$	711	718	694
$\gamma(CC)_C$, $\delta_s(CH_2)$, ν_s(C–N), δ(CCC), δ(OH)	783	788	
			813
			915
$\gamma(CH)_{C/A}$, δ(CCC), $\delta_s(CH_2)$, $\delta_r(CH_3)$, $\nu_{as}(C–O)_E$, δ(OH)	951	953	
$\delta(CH)_A$, δ(CH), $\delta_r(CH_2)$, $\delta(OH)_A$	996	989	
$\delta(CH)_A$, δ(CH), $\delta_w(CH_2)$, $\delta(OH)_A$	1123	1124	
$\delta(CH)_A$, δ(CH), $\delta_s(CH_2)_B$, $\delta(OH)_A$	1199	1188	1182
δ(CH), $\delta(CCC)_C$, $\delta_w(CH_2)_B$, $\delta(OH)_A$	1238		1229
δ(CCC), $\delta(CH)_C$, $\delta_s(CH_2)_D$, $\nu(C–O)_C$	1294	1279	1287
$\delta(CH)_{A/B}$, $\delta_w(CH_2)_B$	1349	1336	1361
$\delta_w(CH_2)_B$, δ(CH)	1379		1368
$\delta_w(CH_2)_D$, $\delta_s(CH_3)_D$, δ(C–OH)	1408	1387	
		1429	
$\delta_{as}(CH_3)_D$	1494	1445	1449
$\delta_s(CH_2)_D$, $\delta_{as}(CH_3)_D$	1525	1472	
		1528	1526
$\nu(CC)_C$, $\delta(CH)_C$, $\delta_w(CH_2)$	1634	1596	1585
$\nu(CC)_C$, $\delta(CH)_C$, $\delta(CH_3)$	1671	1635	1619
$\nu(C=C)_A$	1699	1653	1637

*ν, stretching; δ, bending, γ, out-plane bending, δ_s, scissoring, δ_w, wagging, δ_r, rocking, as, asymmetric.

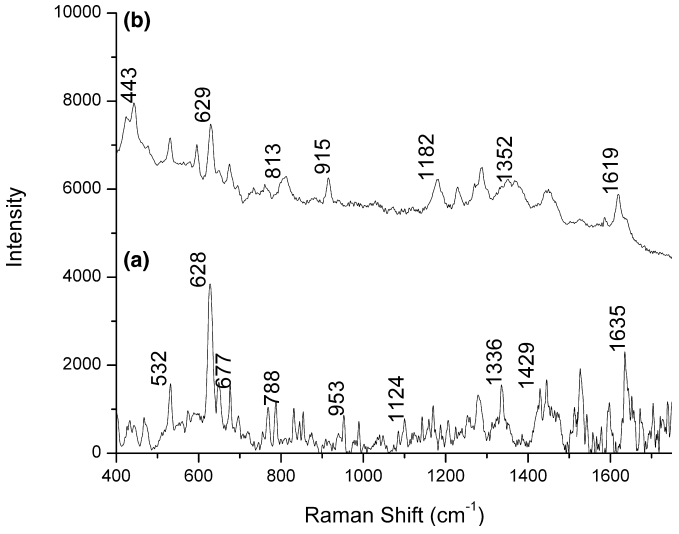

FIG. 5—*Normal Raman (SERDS at 785 nm) (a) and SERS (at 633 nm) (b) spectra of codeine.*

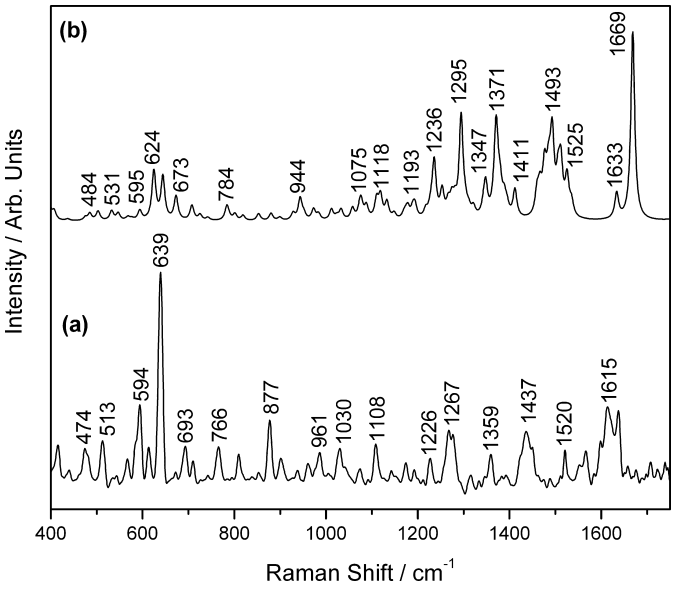

FIG. 6—*Normal Raman (SERDS) (a) and calculated DFT (b) spectra of hydrocodone.*

SERS spectra of codeine were recorded at 785 and 633 nm. As in the case of morphine, the use of the 633 nm laser provides better results to analyze codeine by SERS spectroscopy. The bands in the SERS spectrum are comparable to those seen in the normal Raman spectrum (Fig. 5*a*). As in the previous drug, the main change in the spectrum when the molecule is adsorbed to the Ag surface is the great decrease in intensity of the strongest band in the normal Raman spectrum and its shoulder, at 628 and 650/cm, respectively. These bands mainly involve the out of plane vibration of the hydrogen atoms bonded to the C=C in the ring A. On the other hand, in the high wavenumber region of the Raman spectra, a shift of the bands at 1635 and 1653/cm is seen in the SERS spectrum to 1619 and 1637/cm, respectively, as well as a decrease in relative intensity of those bands in the spectrum when the Ag colloid is used. These facts suggest an interaction of codeine with the Ag surface by the double bond in ring A, which is the same configuration deduced for morphine.

When using a silver surface formed photolytically by the probe laser as the SERS substrate (13) the most intense band in the 900–1750/cm region is seen at 1032/cm. A group of four medium intensity bands around 1600/cm is also shown in the SERS spectrum of codeine. On the contrary, when the Ag colloids are used, a very weak band is seen at 1027/cm, and only a couple of bands appear in the 1600/cm region. These differences can be attributed to the different type of SERS substrate used in the two experiments. Therefore, a different adsorption geometry of codeine on the Ag surface would be expected and, consequently, a different spectral profile.

In the evaluation of the aggregating agents, we found that only NaCl gives a good spectrum. The SERS spectra using HCL, NaOH, and KNO_3 showed no significant intensity that could be used to carry out a comparison of the spectral band.

Hydrocodone

The main bands shown in the normal Raman spectra (Fig. 6*a*) appear at 513, 594, 639, 877, 1267, 1437, 1615, and 1637/cm. These bands correspond to the following ones in the DFT-calculated spectrum (Fig. 6*b*): 504, 595, 644, 880, 1295, 1493, 1633, and 1669/cm. These values show the very good fit between the experimental and calculated spectra, especially in the most intense region of the spectrum (around 640/cm). As in the previous cases, in the high wavenumbers region, the bands in the DFT spectrum appear at higher values than in the experimental one.

The most intense band in the normal Raman spectrum, at 639/cm, involves deformations of all the rings, including the heterocyclic ones (COC and CNC), out of plane CH and C=O motions and rocking of the CH_2 groups. The nearby band at 594/cm is assigned to $\delta(CH_2)$ (mainly of ring D), γ(CC), γ(CH), δ(C–O), γ(C=O), and δ(CNC). On the other hand, the band at 1267/cm corresponds to δ(CCC), ν(C–O), $\delta(CH_2)$, and δ(CH) while the one at 1493/cm is assigned only to the $\delta(CH_3)$ of the OCH_3 group attached to ring C. The most intense bands in the high wavenumber region, at 1615 and 1637/cm are assigned to ν(CC) of the aromatic ring together with $\delta(CH_2)$ and $\delta(CH_3)$, respectively. The complete assignments of the main bands of the hydrocodone Raman spectrum are listed in Table 3. Unlike the previous two opiates, there has been no reported work on this drug using FT-Raman or dispersive Raman spectroscopy.

As in the case of the other drugs, the SERS spectrum of the hydrocodone obtained at 633 nm (Fig. 7) is of higher quality than that at 785 nm. Even though the SERS spectrum contains the same bands as the normal Raman spectrum, there are some differences between them. The most obvious one is the huge decrease in intensity of the Raman band at 639/cm. On the other hand, in the same region, a relative enhancement of the bands at 514, 568, 583, 615, and 709/cm is observed when the spectrum is recorded on Ag nanoparticles. Another important change is the relative enhancement of the bands at 1189, 1228, 1278, and 1334/cm. However, the bands at 1449, 1616, and 1636/cm maintain approximately the same intensity.

In the case of hydrocodone, it is not clear which part of drug interacts with the Ag. As the bands corresponding to the C ring (in the 1600/cm region) are not affected by the proximity of the surface, the adsorption through the aromatic ring can be ruled out. However, the opiate could interact by the carbonyl or the amine groups in rings A and D, respectively, as the bands involving motions of those groups (640 and 762/cm) are considerably decreased in the SERS spectrum. The interaction by means of the

TABLE 3—*Wavenumbers of the DFT, normal Raman, and SERS spectra of hydrocodone and assignments of vibrational normal modes.*

Description*	DFT	Raman	SERS
		474	478
$\gamma(CC)_C$, $\gamma(CH)_C$, $\delta(COC)$, $\delta_r(CH_2)$	504	513	514
$\gamma(CC)_C$, $\gamma(CH)_C$, $\delta_r(CH_2)$	569	567	568
			583
$\delta_r(CH_2)_D$, $\gamma(CC)_C$, $\gamma(CH)_C$, $\delta(COC)$, $\gamma(C=O)$, $\delta(CNC)$	595	594	595
$\gamma(CC)_C$, $\gamma(CH)_C$, $\delta_r(CH_2)$, $\delta(CCC)$	624	613	615
$\delta(CCC)_C$, $\delta(CCC)$, $\gamma(CH)_C$, $\gamma(C=O)$, $\delta(COC)$, $\delta_r(CH_2)$, $\delta(CNC)$	644	639	640
$\delta(CCC)_C$, $\gamma(CC)_C$, $\delta(COC)$, $\delta_r(CH_2)$, $\gamma(CH)$	673	693	695
$\delta(CCC)_C$, $\gamma(CC)_C$, $\delta(COC)_C$, $\delta_r(CH_2)$, $\delta_r(CH_3)$	707	709	709
$\gamma(C=O)$, $\gamma(CC)_C$, $\delta(CCC)$, $\nu_s(NC)$, $\delta_r(CH_2)_{A/B}$	784	766	762
$\delta(CH)_C$, $\delta_r(CH_2)_D$	818	809	803
$\delta(CCC)$, $\nu(N–CH_3)$, $\delta_r(CH_3)_D$, $\delta_w(CH_2)_B$, $\delta_r(CH_2)_D$	880	877	876
$\delta(CCC)_{A/C/D}$, $\nu_s(C–O)_C$, $\delta_r(CH_2)$	899	901	903
$\nu(COC)_E$, $\delta(CCC)_{A/D}$, $\delta_w(CH_2)_D$, $\delta_r(CH_2)_A$, $\delta_r(CH_3)_D$	973	961	964
$\nu(C–O)_E$, $\delta(CCC)_C$, $\delta_r(CH_3)$, $\delta_r(CH_2)_D$	1034	1030	1027
$\delta(CCC)_A$, $\delta(CH)_C$, $\delta_r(CH_2)_A$	1118	1108	1110
$\delta(CCC)_C$, $\delta_t(CH_2)_B$, $\delta_r(CH_3)_C$, $\delta(CH)$	1193	1173	1189
$\delta(CCC)$, $\delta(CH)$, $\delta_t(CH_2)$, $\nu(C–O)$	1236	1226	1228
$\delta(CCC)$, $\nu_{as}(C–O)$, $\delta_t(CH_2)_A$, $\delta(CH)_C$	1295	1267	1278
$\nu(CC)_C$, $\delta(CH)$, $\delta_w(CH_2)_B$	1371	1359	1350
$\delta_{as}(CH_3)_C$	1493	1437	1449
$\delta_s(CH_2)_D$	1525	1520	1505
		1566	1574
$\nu(CC)_C$, $\delta_w(CH_2)_B$	1633	1615	1616
$\nu(CC)_C$, $\delta_s(CH_3)_C$	1669	1637	1636

*ν, stretching; δ, bending, γ, out-plane bending, δ_s, scissoring, δ_t, twisting, δ_w, wagging, δ_r, rocking, as, asymmetric.

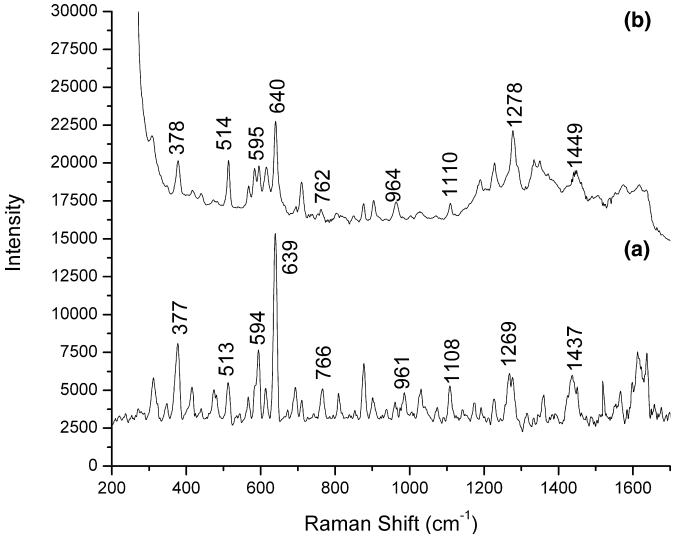

FIG. 7—*Normal Raman (SERDS at 785 nm) (a) and SERS (at 633 nm) (b) spectra of hydrocodone.*

carbonyl group in ring A is more likely due to the higher spatial constraint of the amino group forming ring D.

As in the previous case, aggregation with NaCl gives the best SERS spectrum of hydrocodone. The other aggregating agents showed spectra with no significant bands to use for comparison.

Comparison of the SERS Spectra of the Three Opiates

A comparison of SERS spectra showed that these three compounds can be readily distinguished from each other (Fig. 8).

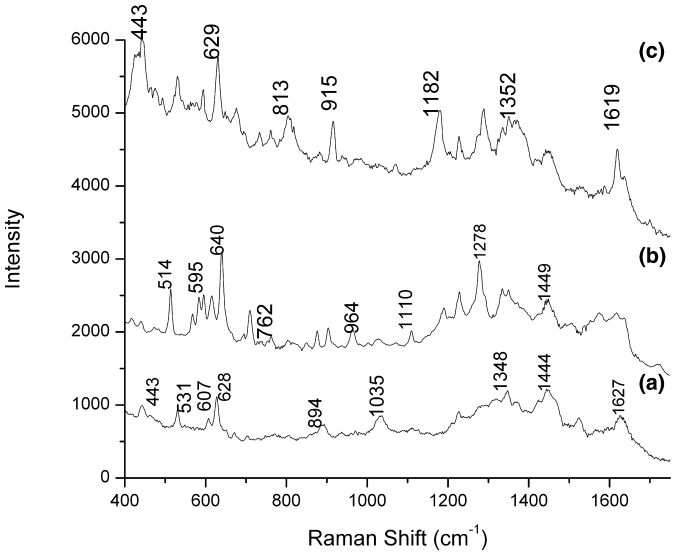

FIG. 8—*SERS spectra of morphine (a), hydrocodone (b), and codeine (c) showing the main discriminant bands of each opiate. Excitation at 633 nm.*

TABLE 4—*Discriminant bands of the SERS spectra of morphine, hydrocodone, and codeine.*

Morphine	Hydrocodone	Codeine
	514	
	568	
	583	
607		
	615	
628		629
	640	
		650
	709	
		734
		813
	876	
889		
	903	
		915
	964	
1035		
1627		

Codeine (Fig. 8*c*) has medium and intense bands at 629, 813, 915, 1182, 1289, and 1619/cm, while morphine (Fig. 8*a*) has its main bands at 628, 1035, 1348, 1444, and 1627/cm. For hydrocodone (Fig. 8*c*), the characteristic bands are at 514, 568, 583, 640, 876, 903, 964, and 1278/cm. These bands alone distinguish between these three drugs. However, to indicate the presence of each opiate in a complex mixture, discriminant bands should be proposed. These bands should have sufficient intensity to be easily observed and not overlap or lie close to intense bands of the other drugs. The discriminant bands proposed to distinguish between morphine, hydrocodone, and codeine are listed in Table 4 and shown in Fig. 8. The region that is most useful in the discrimination is the one around 600/cm, where the most intense bands in all three opiates are found. In hydrocodone, an intense peak is seen at 640/cm but it is complemented with additional bands in the 500–600/cm range, such as 568, 583, and 615/cm. These are not seen in either of the other two drugs. In the same region, codeine may be identified by the very intense band at 629/cm and its shoulder at 650/cm. However, as the strong band overlaps with the most intense band of morphine (628/cm), other bands are necessary to differentiate these compounds. For codeine,

the bands at 734, 813, and 915/cm can be used to identify it. On the other hand, the morphine 628/cm band has a small shoulder band at 607/cm, which is different from both codeine and hydrocodone. Other bands, such as the ones at 889, 1035, and 1627, can be used to confirm the presence of morphine. Therefore, using this region around 600/cm first and then looking at the rest of the spectrum, one should be able to easily distinguish between the three drugs.

Conclusions

Both normal Raman and SERS spectra have been obtained for morphine, codeine, and hydrocodone. The technique used to remove the fluorescence emission from the normal Raman spectra (SERDS), usually gives poor quality spectra of the opiates. This is because of the artifacts introduced by the mathematical operations performed in the spectra. On the contrary, by using the SERS technique, the fluorescence is naturally quenched by the proximity of the Ag nanoparticles, giving rise to good quality spectra without spectral manipulation. The method is found to be stable in that repetition of the procedure produces the identical frequencies and relative intensities. Therefore, it is suitable for identification or qualitative analysis. However, the total intensities observed vary from sample to sample, and therefore at this time, the technique is unreliable for and quantitative measure.

Using the DFT calculations, a comparison was made between the DFT and normal Raman spectra, which enables assignment of the corresponding vibrations to their bands. The interaction between the drugs and the Ag surface was deduced using these assignments. In the case of morphine and codeine, an interaction of the opiate with the nanoparticles occurs through the C=C on ring A. Hydrocodone, which lacks that double bond, is likely to be adsorbed on the Ag by the carbonyl.

Using SERS, it was shown that the three drugs have sufficiently different spectra to differentiate them and to indicate their presence in a mixture of them. Important for forensic purposes, normal Raman and SERS analysis was performed with only 1–2 μL of the 1 mg/mL drug solution and established the sensitivity of these methods for trace amounts of drug samples. Further research should be carried out on the metabolites of these drugs to determine whether they also can be distinguished from their precursors in various biologic matrices.

Acknowledgments

This work was supported by the National Institute of Justice (Department of Justice Award No. 2006-DN-BX-K034) and the City University Collaborative Incentive Program (No. 80209). This work was also supported by the National Science Foundation under Cooperative Agreement No. RII-9353488, Grants No. CHE-0091362, CHE-0345987, and No. ECS0217646. Additionally, it was supported by the City University of New York PSC-BHE Faculty Research Award Program. Scientific research work at the Metropolitan Museum of Art was supported in part by grants from the Andrew W. Mellon Foundation, the David H. Koch Family Foundation, and the National Science Foundation Grant IMR 0526926 (which supplied the Bruker Senterra/Ramanscope combined dispersive Raman/FT-Raman spectrometer).

References

1. Bartick EG. Applications of vibrational spectroscopy in criminal forensic analysis. In: Chalmers JM, Griffiths PR, editors. Handbook of vibrational spectroscopy. Chichester, UK: John Wiley and Sons Ltd., 2002;2993–3004.
2. White P. Surface enhanced resonance Raman scattering spectroscopy. In: Robertson J, Grieve M, editors. Forensic examination of fibers, 2nd edn. New York, NY: Taylor and Francis Group, 1999; 337–42.
3. Birke RL, Lombardi JR. The role of surface roughness in surface enhanced Raman spectroscopy. In: Garetz B, Lombardi JR, editors. Advances in laser spectroscopy, Vol. I. Philadelphia, PA: Heyden, 1982;143–53.
4. Rodger C, Dent G, Watkinson J, Smith WE. Surface enhanced resonance Raman scattering and near-infrared Fourier transform Raman scattering as *in situ* probes of ink jet dyes. Appl Spectrosc 2000;54:567–76.
5. Geiman I, Leona M, Lombardi JR. Application of Raman spectroscopy and surface-enhanced Raman scattering to the analysis of synthetic dyes found in ballpoint pen ink. J Forensic Sci 2009;54(4):947–52.
6. White PC, Munro CH, Smith WE. *In situ* surface enhanced resonance Raman scattering analysis of a reactive dye covalently bound to cotton. Analyst 1996;121:835–8.
7. Ryder AG. Surface enhanced Raman scattering for narcotic detection and application to chemical biology. Curr Opin Chem Biol 2005;9:489–93.
8. Sagmuller B, Schwarze B, Brehm G, Trachta G, Schneider S. Identification of illicit drugs by a combination of liquid chromatography and surface-enhanced Raman scattering spectroscopy. J Mol Struct 2003; 661–662:279–90.
9. Sagmuller B, Schwarze B, Brehm G, Schneider S. Application of SERS spectroscopy to the identification of (3,4-methylenedioxy)amphetamine in forensic samples utilizing matrix stabilized silver halides. Analyst 2001;126:2066–71.
10. Cinta Pinzaru S, Pavel I, Leopold N, Keifer W. Identification and characterization of pharmaceuticals using Raman and surface-enhanced Raman scattering. J Raman Spectrosc 2004;35:338–46.
11. Garrido JMPJ, Marques MPM, Silva AMS, Macedo TRA, Oliveira-Brett AM, Borges F. Spectroscopic and electrochemical studies of cocaine–opioid interactions. Anal Bioanal Chem 2007;388:1799–808.
12. Day JS, Edwards HGM, Dobrowski SA, Voice AM. The detection of drugs of abuse in fingerprints using Raman spectroscopy II: cyanoacrylate-fumed fingerprints. Spectrochim Acta A 2004;60:1725–30.
13. Trachta G, Schwarze B, Sagmuller B, Brehm G, Schneider S. Combination of high-performance liquid chromatography and SERS detection applied to the analysis of drugs in human blood and urine. J Mol Struct 2004;693:175–85.
14. Walsh CT, Schwartz-Bloom RD, editors. Levine's pharmacology drug actions and reactions, 7th edn. New York, NY: Taylor and Francis Group, 2005.
15. Wang M, Teslova T, Xu F, Lombardi JR, Birke RL, Leona M. Raman and surface enhanced Raman scattering of 3-hydroxyflavone. J Phys ChemC 2007;111:3044–52.
16. Teslova T, Corredor C, Livingstone R, Spataru T, Birke RL, Lombardi JR, et al. Raman and surface-enhanced Raman spectra of flavone and several hydroxy derivatives. J Raman Spectrosc 2007;38:802–18.
17. Wang M, Spataru T, Lombardi JR, Birke RL. Time-resolved surface enhanced Raman scattering studies of 3-hydroxyflavone on a Ag electrode. J Phys Chem C 2007;111:3038–43.
18. Leona M, Lombardi JR. Identification of berberine in ancient and historical textiles by surface-enhanced Raman scattering. J Raman Spectrosc 2007;38:853–8.
19. Atkins P, de Paula J. Physical chemistry, 7th edn. New York, NY: W.H. Freeman and Company, 2002.
20. Lee PC, Meisel D. Absorption and surface-enhanced Raman of dyes on silver and golds sols. J Phys Chem 1982;86:3391–5.
21. Campion A, Kambhampati P. Surface-enhanced Raman scattering. Chem Soc Rev 1998;27:241–50.
22. Zhao J, Carrabba MM, Allen FS. Automated fluorescence rejection using shifted excitation Raman difference spectroscopy. Appl Spectrosc 2002;56:834–45.
23. Shreve AP, Cherepy NJ, Mathies RA. Effective rejection of fluorescence interference in Raman spectroscopy using a shifted excitation difference technique. Appl Spectrosc 1992;46:707–11.
24. Maiwald M, Erbert G, Klehr A, Kronfeldt HD, Schmidt H, Sumpf B, et al. Rapid shifted excitation Raman difference spectroscopy with a distributed feedback diode laser emitting at 785 nm. Appl Phys B 2006;85:509–12.
25. Frisch MJ, Trucks GW, Schlegel HB, Scuseria GE, Robb MA, Cheeseman JR. Gaussian 03, Revision C.02, Wallingford, CT: Gaussian, Inc., 2004.

26. Schulz H, Baranska M, Quilitzsch R, Schutze W. Determination of alkaloids in capsules, milk and ethanolic extracts of poppy (*papaver somniferum* L.) by ATR-FT-IR and FT-Raman spectroscopy. Analyst 2004;129:917–20.
27. Li PW, Zhang J, Zhang L, Mo YJ. Surface-enhanced Raman scattering and adsorption studies of morphine on silver island film. Vib Spectrosc 2009;49:2–6.

Additional information and reprint requests:
Maria Vega Cañamares, Ph.D.
Department of Chemistry and Center for Study of Structures and Interfaces (CASI)
The City College of New York
Convent Avenue at 138th Street, New York, NY 10031
E-mail: maria.canamares@metmuseum.org